

AD-A144 825

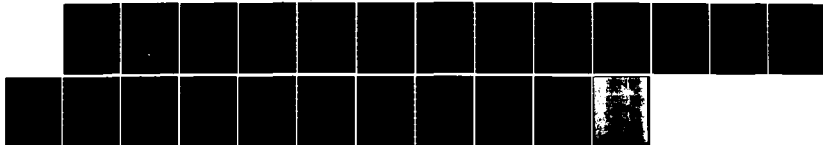
A PROPOSED TECHNIQUE FOR CREATION AND DETECTION OF HOT
ELECTRON IONIZATION. (U) NAVAL RESEARCH LAB WASHINGTON
DC J P APRUZESE ET AL. 19 JUL 84 NRL-NR-5391

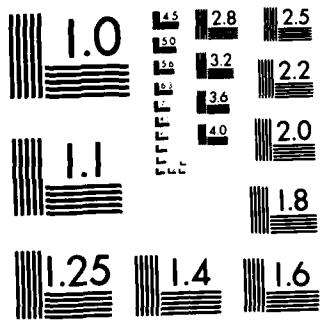
1/1

UNCLASSIFIED

F/G 20/9

NL





MICROCOPY RESOLUTION TEST CHART
NATIONAL BUREAU OF STANDARDS-1963-A

2

NRL Memorandum Report 5391

A Proposed Technique for Creation and Detection of Hot Electron Ionization and Gain Effects in a Laser-Produced Tin Plasma

J. P. APRUZESE AND J. DAVIS

*Plasma Radiation Branch
Plasma Physics Division*

July 19, 1984

This work was supported in part by the Office of Naval Research.



RECEIVED
AUG 6 1984
A

NAVAL RESEARCH LABORATORY
Washington, D.C.

Approved for public release; distribution unlimited.

84 08 03 054

AD-A144 025

DTIC FILE COPY

REPORT DOCUMENTATION PAGE				
1a REPORT SECURITY CLASSIFICATION UNCLASSIFIED		1b RESTRICTIVE MARKINGS		
2a SECURITY CLASSIFICATION AUTHORITY		3 DISTRIBUTION AVAILABILITY OF REPORT		
2b DECLASSIFICATION/DOWNGRADING SCHEDULE		Approved for public release; distribution unlimited.		
4 PERFORMING ORGANIZATION REPORT NUMBER(S) NRL Memorandum Report 5391		5. MONITORING ORGANIZATION REPORT NUMBER(S)		
6a NAME OF PERFORMING ORGANIZATION Naval Research Laboratory	6b OFFICE SYMBOL (If applicable) Code 4720	7a NAME OF MONITORING ORGANIZATION		
6c ADDRESS (City, State and ZIP Code) Washington, DC 20375		7b ADDRESS (City, State and ZIP Code)		
8a NAME OF FUNDING SPONSORING ORGANIZATION Office of Naval Research	8b OFFICE SYMBOL (If applicable)	9 PROCUREMENT INSTRUMENT IDENTIFICATION NUMBER		
8c ADDRESS (City, State and ZIP Code) Arlington, VA 22217		10 SOURCE OF FUNDING NOS.		
		PROGRAM ELEMENT NO 61153N	PROJECT NO	TASK NO RR011-09-41
				WORK UNIT NO DD080-035
11 TITLE (Include Security Classification) (See page ii)				
12 PERSONAL AUTHOR(S) Apruzese, J.P. and Davis, J.				
13a TYPE OF REPORT Interim	13b TIME COVERED FROM TO	14 DATE OF REPORT (Yr., Mo., Day) July 19, 1984	15 PAGE COUNT 23	
16 SUPPLEMENTARY NOTATION This work was supported in part by the Office of Naval Research.				
17 COSATI CODES		18 SUBJECT TERMS (Continue on reverse if necessary and identify by block number)		
FIELD	GROUP	SUB GR		
			X-ray gain enhancement	
			Suprathermal electrons	
			Linearly focused beams	
			Laser-produced tin plasma	
19 ABSTRACT (Continue on reverse if necessary and identify by block number) <p>It has recently been demonstrated that suprathermal electrons, while deleterious to laser fusion, may have significant and beneficial effects in plasma ionization and promoting population inversions in neon-like ions. In this Memorandum Report we consider experimental demonstration of these effects. Using linearly focused and aligned beams, we propose a series of shots with planar tin targets ($Z=50$). At irradiances of $\sim 1-4 \times 10^{14}$ $W\text{ cm}^{-2}$, both the energies and numbers of hot electrons produced by a $1.05\ \mu\text{m}$ laser beam should be appropriate for substantial enhancement of gain in the $3s-3p$ transition of neon-like tin at 118.2\AA. If possible a quiescent plasma should be prepared with an $0.35\ \mu\text{m}$ beam, which would be followed by a $1.05\ \mu\text{m}$ pulse to create a burst of hot electrons at $4-5\ \text{keV}$ to pump the upper lasing state.</p>				
20 DISTRIBUTION AVAILABILITY OF ABSTRACT UNCLASSIFIED UNLIMITED <input checked="" type="checkbox"/> SAME AS RPT <input type="checkbox"/> DTIC USERS <input type="checkbox"/>		21 ABSTRACT SECURITY CLASSIFICATION UNCLASSIFIED		
22a NAME OF RESPONSIBLE INDIVIDUAL J. Davis	22b TELEPHONE NUMBER (Include Area Code) (202) 767-3278	22c OFFICE SYMBOL Code 4720		

SECURITY CLASSIFICATION OF THIS PAGE

11. TITLE (Include Security Classification)

**A Proposed Technique for Creation and Detection of Hot Electron Ionization and Gain Effects
in a Laser-Produced Tin Plasma**

SECURITY CLASSIFICATION OF THIS PAGE

CONTENTS

I. BACKGROUND 1

II. SCALING OF IRON RESULTS TO TIN 5

III. EXPERIMENTAL ACHIEVEMENT OF THE REQUIRED CONDITIONS .. 7

IV. EXPERIMENTAL DIAGNOSTICS 8

ACKNOWLEDGMENTS 10

REFERENCES 18



A1

A PROPOSED TECHNIQUE FOR CREATION AND DETECTION OF HOT ELECTRON IONIZATION AND GAIN EFFECTS IN A LASER-PRODUCED TIN PLASMA

I. BACKGROUND

The production of suprathermal electrons in plasmas driven by high power lasers of wavelengths $\lambda > 1 \mu\text{m}$ has been recognized and studied for nearly a decade. It is generally believed that the resonant absorption mechanism accounts for the bulk of this production of hot electrons.¹ These hot electrons are generally viewed as deleterious to the achievement of laser fusion for two main reasons: first, the penetration of hot electrons results in pellet preheat, inhibiting compression; second, hot electrons are a wasteful channel for the driving laser's energy. They must first be converted to thermal energy to assist the compression process, and the conversion process has proven inefficient.² Some attempts have been made to circumvent these problems, one of the most recent of which involves using return currents driven by the suprathermals to implode cylindrical targets.² The generation of hot electrons, scaling³ as $(I \lambda^2)^{1/2}$ is obviously a more serious problem at high laser irradiance (I) and long wavelengths.

However, the presence of a double-peaked electron energy distribution may be exploitable for purposes other than laser fusion. The production of a population inversion in a plasma is a clear possibility; the presence of a non-thermal electron pool is obviously conducive to peculiar level population distributions.

In recent years considerable study has been devoted to neon-like ions⁴⁻⁸ in the search for plasma conditions which will promote population inversions conducive to lasing in the x-ray region of the spectrum. The attractiveness of the neon-like configuration stems from the fact that the proposed lower lasing level, $1s^2 2s^2 2p^5 3s^1 p_1$, decays rapidly to the closed shell ground state whereas the upper lasing level, $1s^2 2s^2 2p^5 3p^1 s_0$, is by comparison radiatively stable. The simplified energy level diagram of Fig. 1 illustrates the basic inversion mechanism in the case of neon-like iron (Fe XVII).

The gain achievable in such a neon-like ion has recently been shown⁹ to be related to the possible presence of hot electrons. Specifically it has been demonstrated quantitatively that suprathermals such as those produced in high power laser-plasma experiments may be used to substantially enhance gain in 3p-3s transitions of neon-like ions.

Specific calculations were performed using a detailed model of ionized iron. The energy of the suprathermals must be roughly matched to the threshold excitation energy of the (upper) 3p lasing state. For iron, this energy is ~ 800 eV and necessitates the use of low irradiances (2.5×10^{13} Watts cm^{-2} at $\lambda = 1.05 \mu\text{m}$) to increase the gain in the $3s^1P_1 - 3p^1S_0$ transition of Fe XVII, which lies at 254.9 \AA (48.64 eV).

As detailed below, the ratio of hot to cold electrons must be at least a few percent by number for gain enhancements to be significant. At present, the general belief of the laser-plasma community (see Ref. 10 for example) is that such fractions are not achievable at $1.05 \mu\text{m}$ at such a low irradiance as 2.5×10^{13} Watts cm^{-2} . Some measurements^{11,12} contradicting this generally held view have been reported. However, it is felt that higher irradiances are the more prudent choice. Since both the hot electron energy and fraction increase with irradiance, a higher-Z element with a correspondingly higher excitation threshold is required. A reasonable choice both for target fabrication and atomic number is tin ($Z = 50$), whose upper lasing state has an excitation threshold of ~ 4 keV. The corresponding laser irradiance required to produce hot electrons of this energy is a few times 10^{14} Watts cm^{-2} , in a regime where many more hot electrons will be produced. Even though the specific results below are given from our previously developed detailed iron atomic model, the same principles apply to our chosen target element tin. Specific Z-scaling of the results is discussed further below. Complete details of the iron calculation are provided in Ref. 9; in this Memorandum Report we concentrate on the relevant results.

First, an extensive series of gain results was obtained over a wide range of postulated conditions with the restriction that the electron distribution be a single-temperature Maxwellian. Peak gains of only $1-4 \text{ cm}^{-1}$ were found for optimum temperatures of 150-200 eV. Above these temperatures the Fe XVII stage abundance declined substantially, along with the resulting gain.

This is expected since the coronal results of Jacobs et al.¹³ show an abundance peak at 250eV and at higher densities collisions result in a substantially greater excitation state than expected in the low-density coronal limit. Since the ionization potential, I_p , of Fe XVII is 1266eV, our results may be compared to those of Vinogradov et al.⁶ which at $T =$

$I_p/6$ for CaXI show a gain of $1-10 \text{ cm}^{-1}$, depending on the density, for the optically thin case. The reason for the modest gains in both cases is that the upper lasing level is located at an energy above the ground state equal to 4 times the electron temperature. Therefore, less than 5% of the ambient electrons are capable of pumping the upper lasing level. It is for this reason that the addition of a hot electron component is a promising technique for gain enhancement. However, the energy of the suprathreshold component must approximate the excitation energy of the 3p state. We find that a suprathreshold component of 100 keV electrons⁴ primarily provides additional ionization, not pumping of the upper lasing state leading to enhanced gain.

Our steady state results for a hot electron component of energy 800eV (the $2p^5 3p^1 S_0$ level is 788eV above the ground level) are presented in Figs. 2-5. We again emphasize that these iron results are readily scalable to tin experiments and this is discussed below in detail. The dramatic increase in gain with hot electron fraction is shown in Fig. 2. This is due to direct collisional pumping of the $2p^5 3p^1 S_0$ level. Above 10% hots, the neon-like fraction is depleted by the increased ionization but the combination of a cold 70eV thermal reservoir and a monoenergetic 800eV electron component results in a substantial neon-like iron presence over a wide ratio of hots to colds. Note that the gain continues to rise even after the neon-like fraction has peaked; this is due to the increasing number of pump electrons. A peak gain of $\sim 40 \text{ cm}^{-1}$ is expected for a hot electron density of 10^{20} cm^{-3} and a cold electron density of $4 \times 10^{20} \text{ cm}^{-3}$. At higher ratios of hot electrons, ionization lowers the gain. The neon-like stage fraction depends sensitively on the hot electron ratio to colds.

Figure 3 displays the sensitivity of the steady-state gain to cold electron temperature. For this calculation, the ratio of hots to colds was fixed at 0.15, and the cold electron density at $4 \times 10^{20} \text{ cm}^{-3}$. The hot electron energy was assumed to be 800eV. Substantial gain is present at cold electron temperatures between 30eV and 100eV, indicating only a moderate sensitivity to this quantity. At higher temperatures ionization lowers the gain as seen by the decrease of the neon-like fraction (also plotted in Fig. 3). At the lower temperatures in this range the gain is somewhat less than the peak. This is due entirely to increased population of the lower lasing level - the upper level is unchanged in population (as

might be expected) since the 800eV hot electrons are still present. The increased population of the lower level results from increased collisional de-excitation to this level from higher excited levels due to the higher cross-sections for these de-excitations at lower electron energies.

Figure 4 demonstrates the dependence of gain on cold electron density. Above $N_e = 3 \times 10^{21} \text{ cm}^{-3}$ the gain is negligible due to the tendency of collisional processes - stronger at high densities - to establish thermal, rather than inverted, population distributions. At lower densities the reduced number of lasing ions also reduces the expected gain. Note, however, that gains in excess of 10 cm^{-1} are predicted for the quite wide range $7 \times 10^{19} < N_e < 3 \times 10^{21} \text{ cm}^{-3}$.

Even with the beneficent presence of hot electrons assumed, the steady-state gain achievable is still limited by ionization of the neon-like ionic stage to the fluorine-like and higher stages. This effect is clearly demonstrated in Fig. 2 by the decrease of both the gain and neon-like fraction as the hot electron fraction increases past 25% by number. This fact suggests that even higher gains are obtainable if a semi-quiet plasma were subjected to a "burst" of hot electrons. In such a situation, a large gain length might well build up for larger hot electron ratios before ionization becomes fully effective in reducing the gain.

Such speculation is confirmed by the results presented in Fig. 5. In this case a numerical experiment was performed wherein a steady-state plasma of cold (background) electron density $4 \times 10^{20} \text{ cm}^{-3}$ is disturbed by the injection of a monoenergetic hot electron pulse of energy 0.8 keV whose density is gaussian in time. The full-width-half-maximum of this pulse was 80 ps, and the hot electron density was assumed to peak at $4 \times 10^{20} \text{ cm}^{-3}$, equal to the background electron density. The injection of the hot electrons in a transient pulse takes advantage of the finite ionization time and allows the small-signal gain to approach 180 cm^{-1} . During the transient period there are plenty of neon-like ions to pump plus a large density of pumping electrons. Ionization eventually reduces the gain.

The actual distribution of hot electrons which will be encountered in laser-produced plasmas is almost certainly not monoenergetic, and will vary with position and time. If the distribution of hot electrons is assumed strictly Maxwellian, we have found that very little steady state gain is achievable due to the tendency of the high energy tail of the hot

electrons' Maxwellian to directly ionize the neon-like state, whose ionization potential from the ground state is just 1.6 times the excitation threshold of the upper lasing state. Steady state gains are obtainable for any hot electron distribution which confines the bulk of the hot electrons within a factor 1.3 of the excitation threshold. The range of parameter space to be explored with reference to exactly which forms of electron distributions optimize gain is prohibitively large for the present. Large transient gains are obtainable for strictly Maxwellian hot electron distributions, however.

The above considerations suggest the use of short driving laser pulses in testing the above concepts. Fortuitously, it is just such pulses which encourage steep density gradients and the accompanying enhanced production of suprathermal electrons.^{11,14}

II. SCALING OF IRON RESULTS TO TIN

It is well known that the hot electron energies obtained in laser-plasma experiments increase as $(I\lambda^2)^\alpha$ where α is somewhat uncertain, probably lying¹⁵ between 0.3 and 0.43. Ref. 3 presents a detailed collection of experimental data which suggests that for a characteristic hot electron energy of 0.8 keV, optimum for iron, irradiances of $I \approx 2-4 \times 10^{13}$ Watts cm^{-2} are required for a laser wavelength $\lambda = 1.05 \mu\text{m}$. As explained above, it is generally believed that the hot electron fraction generated at this irradiance and 1.05 μm wavelength will be considerably less than 1%. For this reason we consider tin ($Z=50$) as a more promising experimental target. We have employed the Hartree-Fock atomic structure code of R. D. Cowan¹⁶ to calculate critical transition probabilities and energies for this element.

The excitation threshold of the upper lasing state is 4 keV, requiring, according to Ref. 3, an irradiance of $\sim 3 \times 10^{14}$ Watts cm^{-2} . The results of Ref. 12 suggest that half to three quarters of the absorbed energy will appear as suprathermals at this irradiance. However, most workers have found a considerably smaller conversion than this at a few times 10^{14} Watts cm^{-2} . Hot electron fractions of at least several percent and probably more for short pulses are expected³, however, in this higher-power regime.

Ionization and excitation energies generally scale approximately as Z_s^2 where Z_s , the screened nuclear charge, is 17 for neon-like iron and 41 for neon-like tin. This expected factor of $(41/17)^2 = 5.8$ for the ratio of characteristic tin-to-iron energies turns out to be slightly high; the actual scaling is very close to 5.0. Therefore, optimum cold electron temperatures for gain are $\sim 5 \times 70 = 350$ eV. Approximate numerical results for tin are obtainable by multiplying the temperatures in the figures by 5.

The scaling of the gain coefficient is slightly more complicated. We find generally that the gain obtained with neon-like iron is approximately 60% of that which would prevail if the lower lasing line state had zero population. Let us assume this same ratio prevails for neon-like tin. It is also found that the upper lasing level $2p^5 3p^1 S_0$ is both populated and depopulated collisionally at densities where significant gain occurs, and that the fractional population of this level for $N_{HOT}/N_{COLD} = 0.15$ at such densities is 7×10^{-4} . The collision rates scale approximately⁶ as Z_s^{-3} ; therefore the same rates as iron will prevail for electron densities a factor of $\sim (41/17)^3 = 14$ higher for tin than for iron. Thus, approximate numerical results for tin are obtainable by scaling the densities in the figures up by this factor of 14. At such densities the gain at line center for a Doppler profile - assumed to be 60% that of a plasma with zero population - of the lower lasing state, is

$$g \text{ (cm}^{-1}\text{)} = 0.6 (1.63 \times 10^{-32}) N_I f \lambda^3 \left(\frac{M}{T_I}\right)^{1/2} A. \quad (1)$$

In Eq. (1) above, N_I is the ion density, f is the fraction of all ions in the upper lasing level ($\sim 7 \times 10^{-4}$), λ is the lasing transition wavelength in Å (118.2), M the ion mass in amu (118.7 for tin), T_I the ion temperature (~ 350 eV, equal to the optimum electron temperature), and A is the spontaneous decay probability of the lasing transition ($3.6 \times 10^{10} \text{ sec}^{-1}$). If $N_e = 4 \times 10^{20} \text{ cm}^{-3}$ for iron, for tin the corresponding optimum N_e is 14 times this value ($5.6 \times 10^{21} \text{ cm}^{-3}$), resulting in $N_I \approx 5.6 \times 10^{21} / 40 \approx 1.4 \times 10^{20} \text{ cm}^{-3}$. Substituting into Eq. (1) we find that $g = 33.2$ under these conditions, compared to 35 cm^{-1} for iron (Fig. 5). Since the

quantities in Eq. (1) are fixed atomic parameters, it is reasonable to conclude that the gain of tin and iron will be about equal for the range of densities and temperatures, scaled by 14 and 5 respectively, presented in the figures. A more detailed study of this gain scaling should be conducted as a comprehensive atomic model for tin is developed.

III. EXPERIMENTAL ACHIEVEMENT OF THE REQUIRED CONDITIONS

We conclude from the above considerations that achievement of substantial gain in neon-like tin requires the following plasma conditions: background thermal electron temperature of 150-700 eV, characteristic hot electron energy of ~ 4 keV - which fixes the laser irradiance at $1-4 \times 10^{14}$ Watts cm^{-2} , and thermal electron densities of $1 \times 10^{21} \text{ cm}^{-3} - 3 \times 10^{22} \text{ cm}^{-3}$, with a hot electron fraction of at least several percent by number. As discussed above the required hot electron densities and energies can be obtained with the above-cited $1.05 \mu\text{m}$ laser irradiances. To evaluate the achievability of the required background conditions we consult detailed experimental studies and modeling^{10,14,17} at similar irradiances for moderate-to-high Z planar targets.

Experiments have been performed at irradiances of 3×10^{14} Watts cm^{-2} at both $1.05 \mu\text{m}$ and $0.53 \mu\text{m}$, and the results have been extensively diagnosed as well as analyzed with LASNEX modeling. The $0.53 \mu\text{m}$ work¹⁴ is relevant in that evidence for the laser wavelength scaling of the plasma profiles was obtained, in particular the electron temperature near the critical surface scales as $\lambda^{0.9}$. Figure 3 of Ref. 10 and Fig. 2 of Ref. 17 are most relevant. Figure 3 of Ref. 10 demonstrates that the required electron densities and temperatures are obtainable $\sim 30-60 \mu\text{m}$ above the original face of the target at 3×10^{14} Watts cm^{-2} . Ref. 17 shows that, for $\lambda = 1.05 \mu\text{m}$ and $I = 1-5 \times 10^{14}$ Watts cm^{-2} , tungsten ($Z=74$) is stripped to at least the nickel-like (28 electron) stage. Stripping these 46 electrons from tungsten requires 41 keV per ion. Stripping 40 electrons from tin to create the neon-like stage requires 40 keV per ion, and is therefore clearly feasible in such experiments. The temperature of the tenuous outer corona is evidently still controversial. Ref. 17 contains a coronal temperature diagnosis of 200-400 eV for tungsten-glass targets; under

similar conditions Ref. 10 obtains T_e in the multi-kilovolt range with gold targets - which are even more efficient radiators. This is of little consequence for our purposes since we are interested in the regions much closer to the critical surface.

Our proposed experimental strategy would be to utilize short pulses to enhance both hot electron production and the possibility of large transient gains. A quiescent plasma should be prepared with an initial short (~100 ps) pulse, preferably at 0.35 μm . The 0.35 μm pulse would minimize both initial hot electron production and the temperature near the critical surface; the 1.05 μm pulse could follow with a variable delay to create the requisite burst of hot electrons. By using both wavelengths, varying the irradiance and the time delay between pulses, one could "bracket" the required conditions so one or more of the shots would be likely to reproduce very closely the optimum conditions. The basic focal spot could be achieved by line focusing UV and IR beams to a total spot of ~ 100 μm x 2500 μm . As detailed below, significant gain should be detectable from such an elongated plasma.

IV. EXPERIMENTAL DIAGNOSTICS

As is evident from Figs. 2 and 3, the relative number of fluorine-like and neon-like ions plays a critical role in determining gain and is very dependent upon the hot electron fraction and the cold electron temperature. Determination of the ionization state of the plasma would be essential in any meaningful analysis of the proposed experiments, and will be useful in clarifying both the role and amounts of hot electrons present.

To determine the ionization state of the plasma, a very useful line ratio has been identified from the calculations described above. The ratio of the intensity of the fluorine like resonance line $2p^5 2p_{3/2} - 2p^4 3s^2 S_{1/2}$ (15.21 Å iron, 3.183 Å tin) to that of the neon-like resonance line $2p^6 1s_0 - 2p^5 3s^3 P_1$ (17.051 Å iron, 3.492 Å tin) sensitively reflects the ratio of fluorine-like to neon-like ions. Figs. 6 and 7 present this dependence for iron upon both hot electron fraction and cold electron temperature. Approximately the same dependence is expected for tin, with the densities scaled upward by a factor of 14 and the temperatures by a

factor of 5. For a hot electron fraction of 7.5%, a cold electron temperature of 350 eV, and density $5.6 \times 10^{21} \text{ cm}^{-3}$, we calculate the emissivity of the neon-like diagnostic line at 3.492 Å to be 20 J/nsec for the plasmas expected to be produced with our proposed focal spot. This is readily detectable and typical of the yields from K-shell argon lines¹⁸ produced in microballoon implosions, whose wavelengths are very similar. The somewhat smaller intensities expected from the fluorine-like diagnostic line are still easily detectable and quantifiable. The cold electron temperature may also be diagnosed from continuum slope measurements coupled with detailed opacity modeling.

Our second objective is the detection of gain at 118.2 Å. To achieve this, spectrometers covering the wavelength region could be aligned both parallel and perpendicular to the elongated plasma. If gain is present, the intensity of this line should be substantially greater when viewed "end-on". Let g be the gain coefficient and S the line source function, assumed uniform. If the plasma is characterized by a width w and length l (in cm), the intensity along the length will be $S(e^{gl}-1)$ and along the width $S(e^{gw}-1)$, resulting in a length-to-width intensity ratio $(e^{gl}-1)/(e^{gw}-1)$. Assume for the moment that the plasma shape parallels that of the focused beam: 0.01 cm x 0.25 cm ($w = 0.01$, $l = 0.25$). For a gain coefficient of 3 cm^{-1} , which should be readily achievable, the ratio of the line intensity parallel to the length to that perpendicular to the length will be $(e^{0.75}-1)/(e^{0.03}-1) \approx 37$. By contrast if no gain exists and instead we have an absorption optical depth of 1 cm^{-1} the ratio is easily found through elementary radiative transfer theory as

$$(1-e^{-0.25}) / (1-e^{-0.01}) \approx 22.$$

Thus factor-of-two accuracy in this ratio will permit the detection of gain of $\sim 3 \text{ cm}^{-1}$ as differentiated from a relatively small amount of absorption. Detection of larger gains would be much easier. For both the line ratio and the gain diagnostics, the spectrograph slit will be oriented in such a fashion as to provide spatial resolution in the direction perpendicular to the target surface. Thus, gain and ionization, reflecting density variations and hot electron penetration, can be monitored spatially.

We reemphasize that a detailed analysis of the actual experimental results using a tin model similar to the iron model described in Reference 9 is crucial. Only in this fashion may quantitative deductions be obtained through theoretical reproduction of the acquired tin spectra. Of equal importance, if unexpected results are obtained, such detailed modeling is virtually required to determine the physical cause of such anomalies. Of course, the more complete modeling effort would involve the self-consistent solution of the equations of radiation hydrodynamics for a proper assessment of temperature and density gradient, shape, and size of the important interaction region.

ACKNOWLEDGMENTS

The authors are grateful to Dr. Allan Hauer of Los Alamos National Laboratory for several very valuable discussions concerning both the experimental constraints and possibilities. This work was supported in part by the Office of Naval Research.

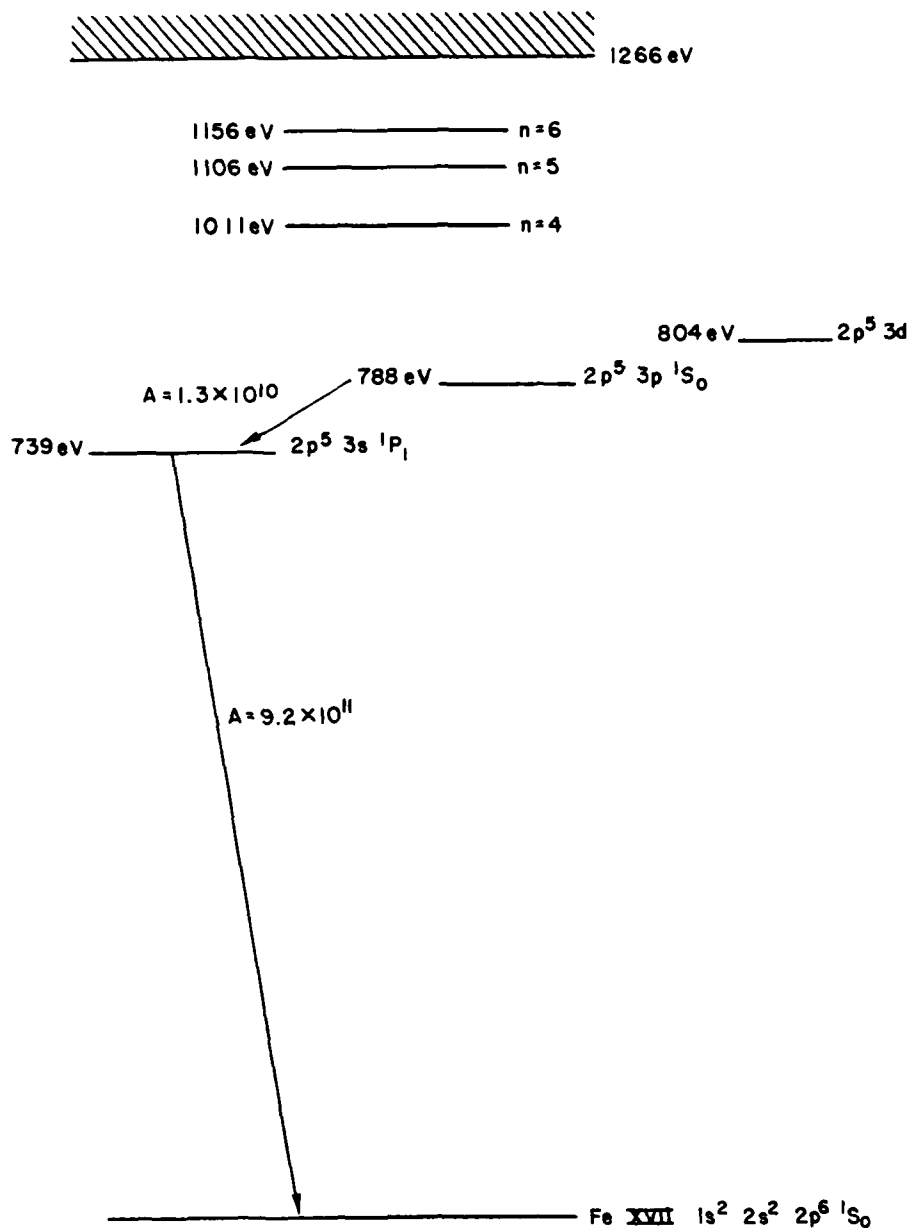


Fig. 1. Simplified energy level structure for neon-like Fe XVII, illustrating the rapid decay of the lower lasing state to ground, and the much slower decay of the upper lasing state. For this and the other Figures, approximate results for tin may be obtained by scaling the iron densities upward by a factor of 14 and the temperatures by a factor of 5.

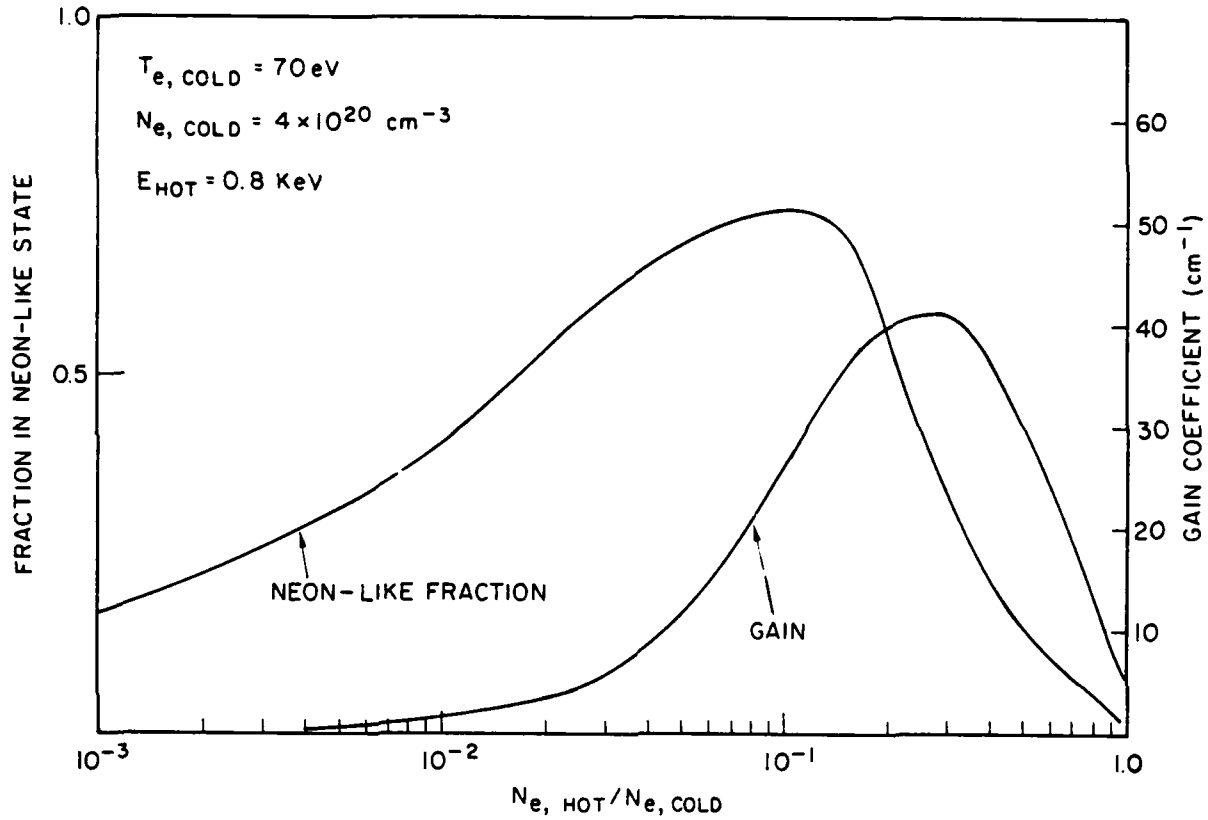


Fig. 2. The steady state gain in the Fe XVII $2p^5 3s^1 P_1 - 2p^5 3p^1 S_0$ transition is plotted as a function of the ratio of 800 eV monoenergetic electrons to 70 eV thermal electrons, for the indicated plasma conditions. The fraction of all ions in the neon-like stage is also shown.

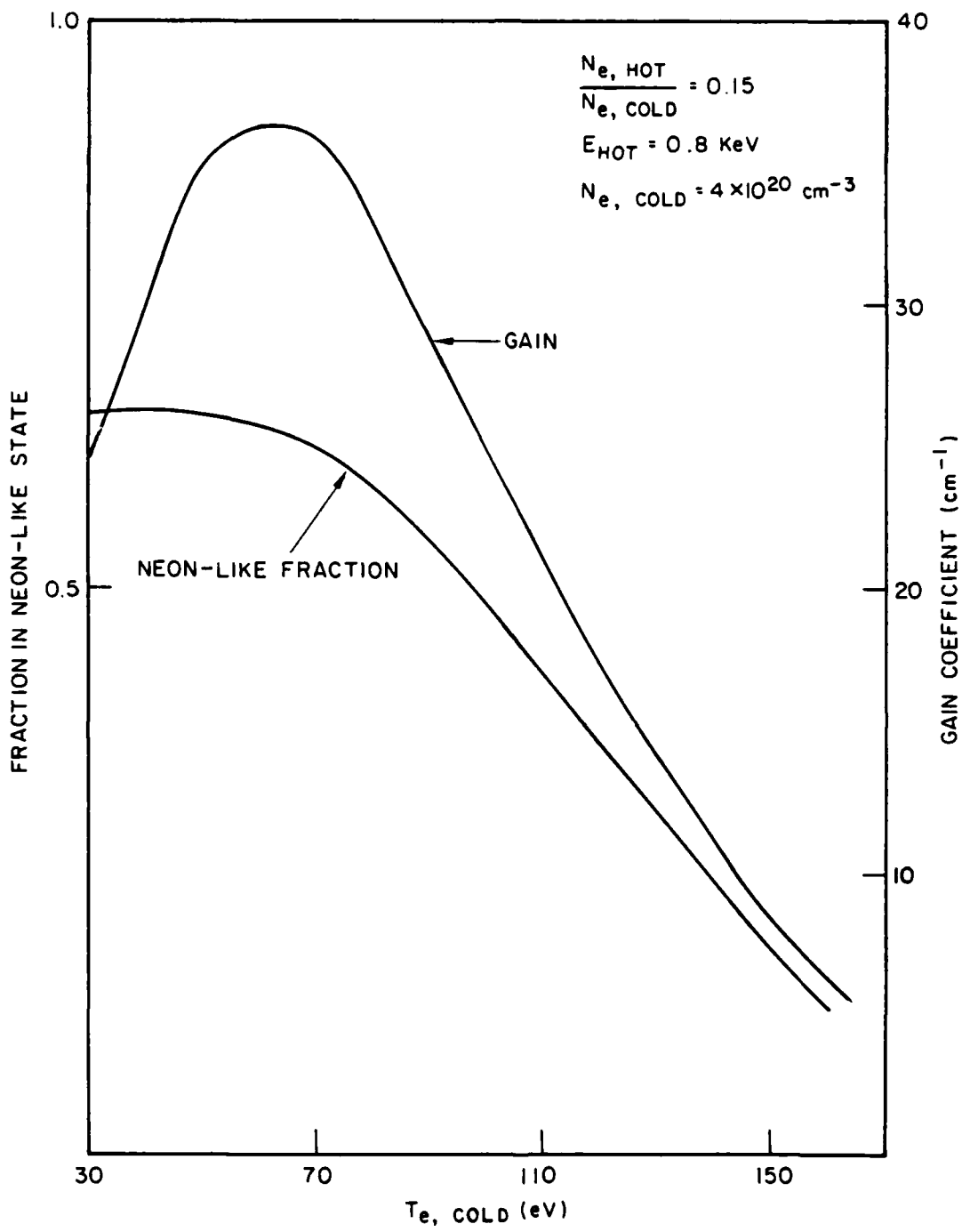


Fig. 3. The steady state gain coefficient in the lasing transition of Fig. 1 is displayed along with the fraction of all ions in the Fe XVII state, as a function of cold electron temperature. Other plasma conditions are as indicated.

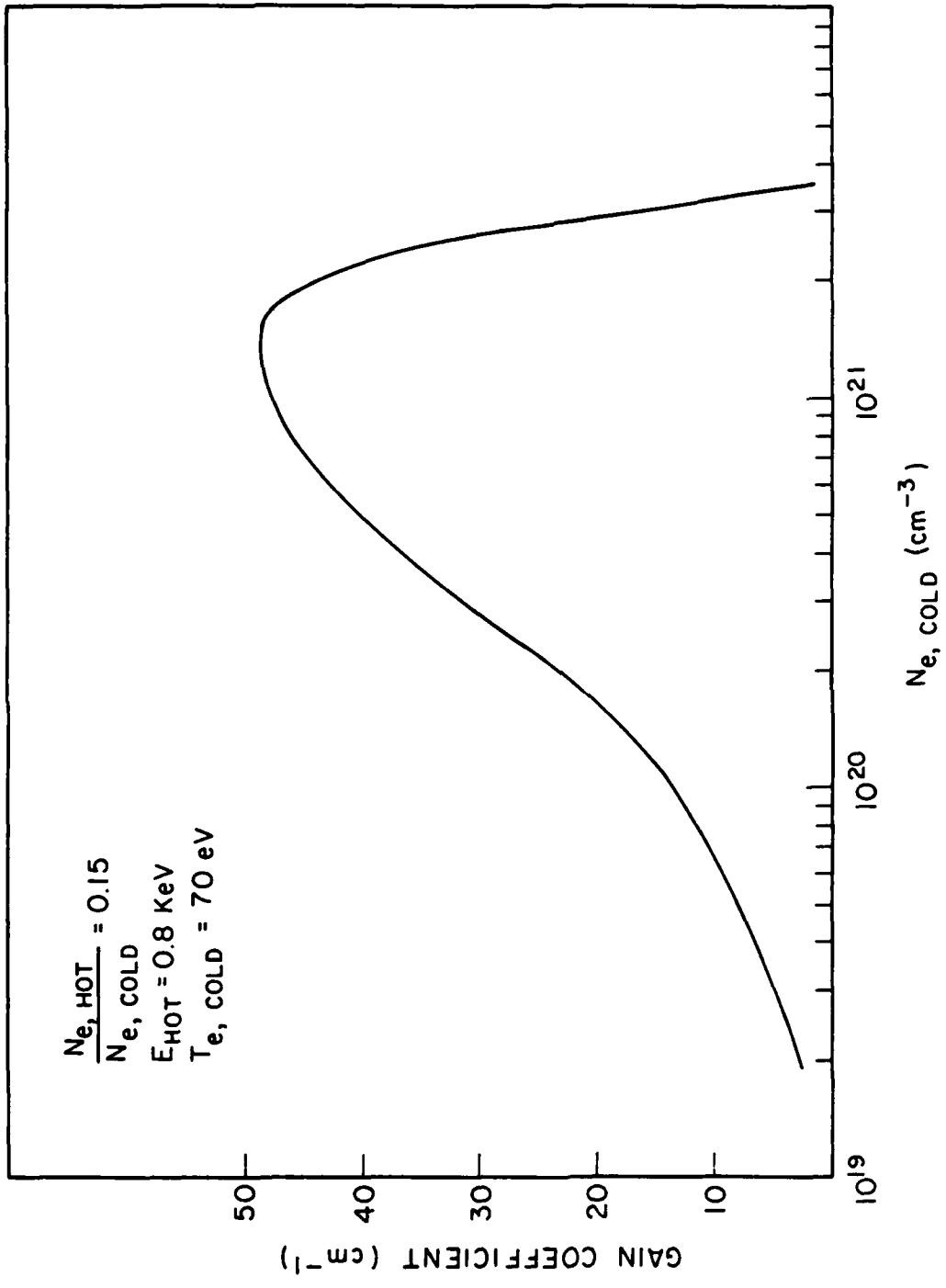


Fig. 4. The steady state gain coefficient is plotted against cold electron density for the indicated plasma conditions.

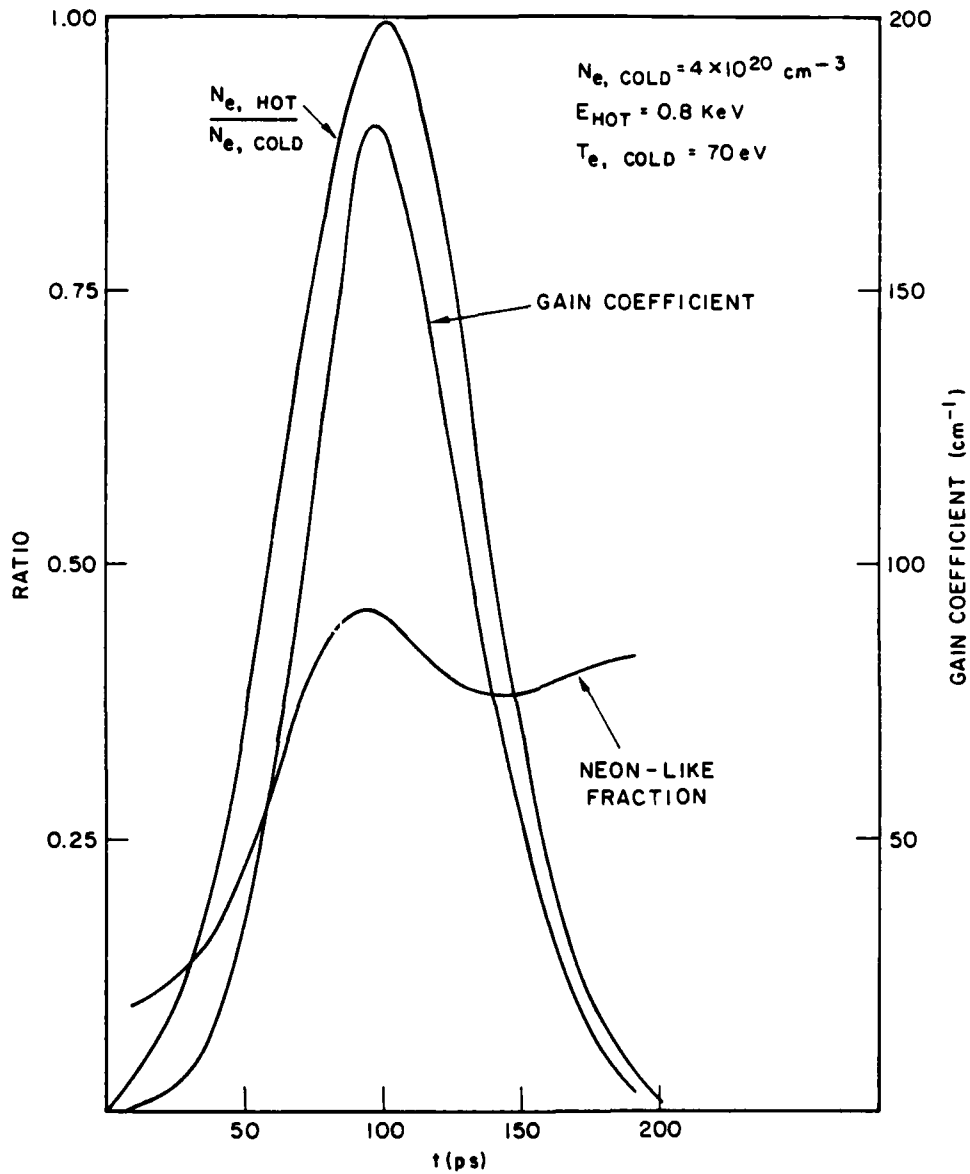


Fig. 5. The time dependent gain coefficient for the lasing transition of Fig. 1 is plotted along with the neon-like ionic fraction and ratio of 800 eV to 70 eV background electrons. A steady state plasma is assumed at the hot electron pulse onset with a cold electron density of $4 \times 10^{20} \text{ cm}^{-3}$.

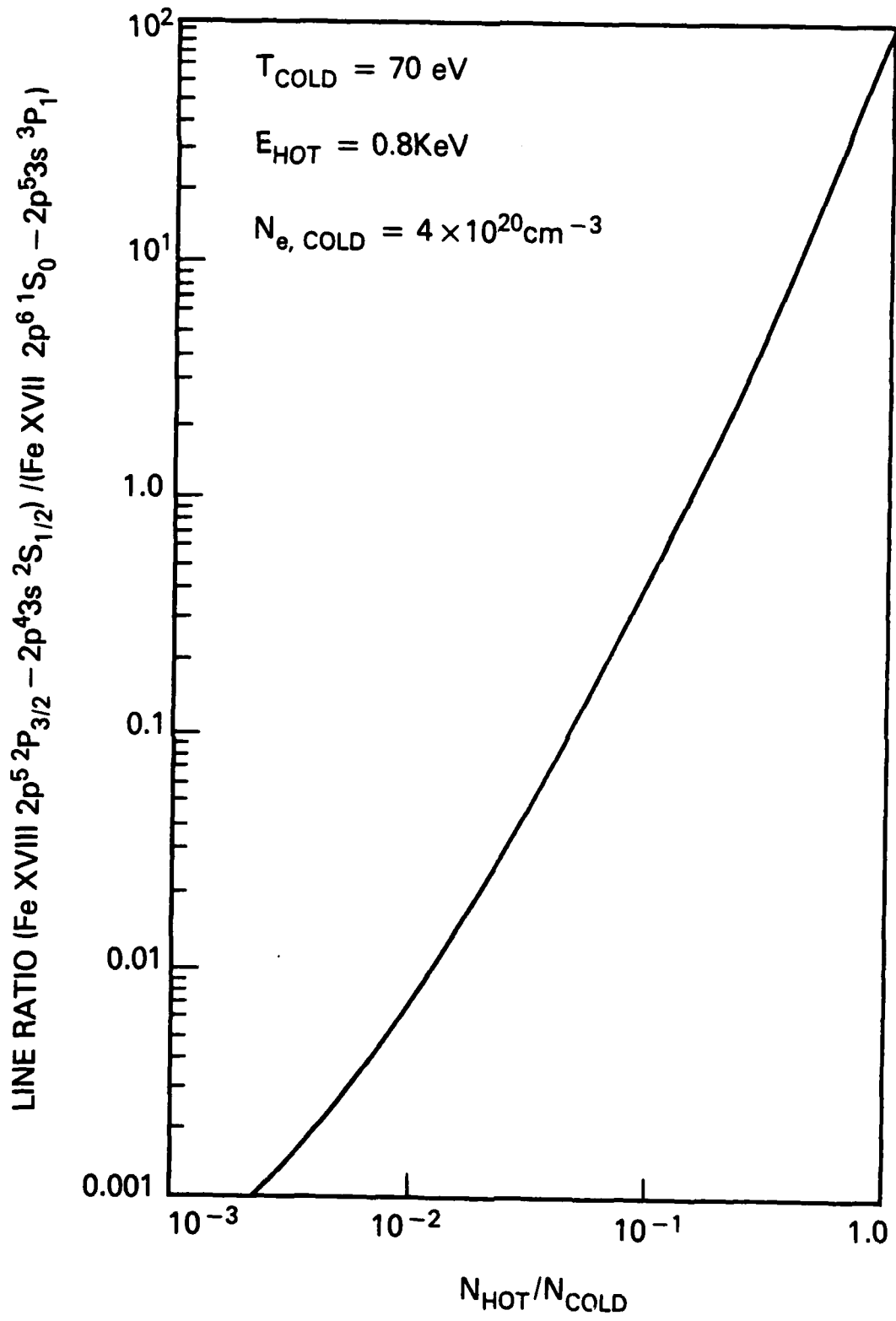


Fig. 6. Fluorine-to-neon-like iron line ratio vs. hot electron fraction for the indicated conditions.

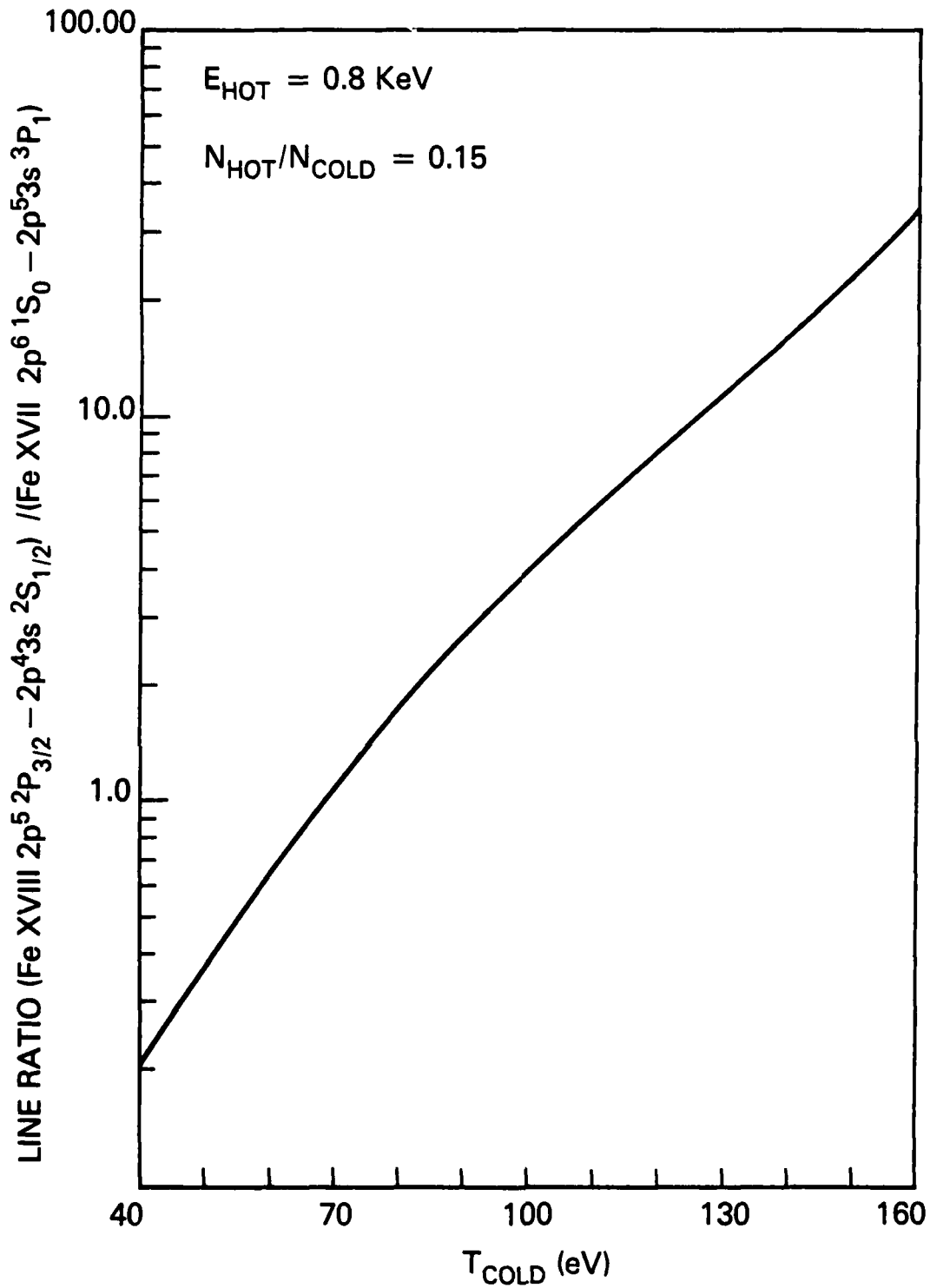


Fig. 7. Fluorine-to-neon like line ratio vs. cold electron temperature for the indicated conditions.

References

1. P. Kolodner and E. Yablonovitch, Phys. Rev. Lett 37, 1754 (1976).
2. A. Hauer and R. J. Mason, Phys. Rev. Lett. 51, 459 (1983).
3. D. W. Forslund, J. M. Kindel, and K. Lee, Phys. Rev. Lett. 39, 284 (1977).
4. R. C. Carman and G. Chapline, in Proceedings of the International Conference on Lasers '81 (STS Press, McLean, Va.) p. 173.
5. A. N. Zherikhin, K. N. Koshelev, and V. S. Letokhov, Kvant. Electron (Moscow) 3, 152 (1976) [Sov. J. Quantum Electron 6, 82 (1976)].
6. A. V. Vinogradov, I. I. Sobel'man, and E. A. Yukov, Kvant. Electron. (Moscow) 4, 63 (1977) [Sov. J. Quantum Electron. 7, 32 (1977)].
7. L. A. Vainshtein, A. V. Vinogradov, U. I. Safronova, and I. Yu. Skobelev, Kvant. Electron. (Moscow) 5, 417 (1978) [Sov. J. Quantum Electron. 8, 239 (1978)].
8. U. Feldman, A. K. Bhatia, and S. Suckewer, J. Appl. Phys. 54, 2188 (1983).
9. J. P. Apruzese and J. Davis, Phys. Rev. A 28, 3686 (1983).
10. M. D. Rosen, et al., Phys. Fluids 22, 2020 (1979).
11. J. E. Balmer and T. P. Donaldson, Phys. Rev. Lett. 39, 1084 (1977).
12. J. A. Tarvin, W. B. Fechner, J. T. Larsen, P. D. Rockett, and D. C. Slater, Phys. Rev. Lett. 51, 1355 (1983).
13. V. L. Jacobs, J. Davis, P. C. Kepple, and M. Blaha, Astrophys. J. 211, 605 (1977).
14. W. C. Mead et al., Phys. Fluids 26, 2316 (1983).
15. R. J. Harrach and R. E. Kidder, Phys. Rev. A 23, 887 (1981).
16. R. D. Cowan, Phys. Rev. 162, 54 (1967); J. Opt. Soc. Am. 58, 808 (1968).
17. H. D. Shay, et al., Phys. Fluids 21, 1634 (1978).
18. A. Hauer, K. G. Whitney, P. C. Kepple, and J. Davis, Phys. Rev. A 28, 963 (1983).

END

FILMED

84

1110